BABEŞ-BOLYAI UNIVERSITY CLUJ-NAPOCA
FACULTY OF PHYSICS
BIOPHYSICS AND MEDICAL PHYSICS

DISSERTATION THESIS

Coordonatori științifici:

Prof. dr. Nicolae Leopold

Lect. Dr. Ștefania –Dana Iancu

Drd. Alexandra Chiriac

Absolvent:

Miruna Alexandra Ibrian

Cluj-Napoca

2025

BABEŞ-BOLYAI UNIVERSITY CLUJ-NAPOCA
FACULTY OF PHYSICS
BIOPHYSICS AND MEDICAL PHYSICS

DISSERTATION THESIS

Analysis of radiative enhancement on metallic surfaces for SERS biosensing optimization

Scientific Coordinator:

Prof. dr. Nicolae Leopold

Lect. Dr. Ștefania –Dana Iancu

Drd. Alexandra Chiriac

Student:

Miruna Alexandra Ibrian

Cluj-Napoca

2025

Contents

Abstract

Metallic-based biosensors have garnered significant attention in recent years due to their multifunctional roles in molecular detection. This study investigates the influence of localized surface plasmon resonance (LSPR), surfactant type, and nanoparticle (NP) surface charge on the adsorption mechanisms of analyte molecules onto silver nanostructures, which is crucial for Surface-Enhanced Raman Scattering (SERS)-based biosensors.

To explore these interactions, colloidal silver nanoparticles exhibiting LSPR peaks at 390 nm, 520–530 nm, and 600–630 nm were synthesized using sodium borohydride ($NaBH_4$) as a reducing agent, hydrogen peroxide (H_2O_2) for LSPR tuning, and trisodium citrate dihydrate as a stabilizer. Additionally, silver nanoparticles (AgNPs) with an LSPR around 420 nm were prepared using established synthetic protocols involving various surfactants, including citrate, glucose, boric acid, and polyethylene glycol (PEG), to assess their compatibility with the target analytes. The analytes investigated were Alizarin Yellow (anionic) and Nile Blue chloride (cationic), and SERS spectra were recorded using a Renishaw Raman spectrometer equipped with 532 nm and 633 nm laser excitation lines.

Among all nanoparticle types tested, those with an LSPR at 390 nm consistently exhibited the highest SERS enhancement for both anionic and cationic molecules. This was observed even though the excitation lasers at 532 nm and 633 nm did not directly match this LSPR. For Alizarin Yellow, SERS spectra were obtained simply by mixing the molecule with the nanoparticles. However, signals were only detected when using the 532 nm laser and nanoparticles with LSPR at 390 nm(yellow) and 600–630 nm(indigo), while no SERS effect was observed with those at 520–530 nm(red).

In the case of Nile Blue chloride, the SERS signals were only observed when nanoparticles exhibiting an LSPR at 390 nm were employed and excited using the 532 nm laser. For other nanoparticles, fluorescence was the dominant signal, indicating that Nile Blue chloride did not adsorb onto their surfaces. Notably, the introduction of calcium (Ca^{2+}) and chloride (Cl^-) ions resulted in fluorescence quenching and the emerge of the SERS signal, likely due to enhanced adsorption of Nile Blue chloride.

Furthermore, the study examined the role of surfactants in SERS performance when nanoparticles shared similar LSPR values. The limit of detection (LOD) varied depending on the surfactant type, with different effects observed for anionic and cationic molecules.

The lowest LOD was achieved with glucose as the surfactant, followed by boric acid, PEG, and finally citrate.

Overall, our findings demonstrate that nanoparticles with an LSPR at 390 nm consistently provide superior SERS enhancement for both anionic and cationic molecules, regardless of the laser excitation wavelength. Additionally, surfactants significantly influence molecular detection at low concentrations, as their displacement by analytes depends on charge interactions. Among the surfactants studied, glucose was the easiest to replace, followed by boric acid, PEG, and citrate. These insights contribute to refining SERS detection protocols for improved analytical sensitivity.

Introduction

Biosensors are becoming increasingly vital in modern medicine, providing tools to observe and predict a patient's health by monitoring biomarkers in biological fluids. Accurate analysis of these biomarkers is essential for healthcare providers to predict disease progression and implement appropriate treatments. Surface-enhanced Raman scattering (SERS) biosensors have emerged as promising analytical tools in the biomedical field due to their high sensitivity and ability to detect molecules at the single-molecule level. SERS biosensors can address current limitations in studying cells and extracellular vesicles (EVs) through plasmon-enhanced electric field and chemical mechanisms. These biosensors enable non-invasive, ultra-sensitive detection using small sample volumes, even with low signal-to-noise ratios, and offer multiplexing capabilities. With their unique ability to reveal molecular signatures, SERS biosensors have the potential to revolutionize disease detection and monitoring, particularly in severe conditions, like cancer, as well as the evaluation of treatment response. Their high sensitivity and multiplex detection capabilities make them ideal for developing fast, effective, and reliable assays to determine biomarker activity and concentration in patient samples. [1]

The development of SERS for widespread, practical application faces several challenges, primarily related to cost, complexity, and real-world applicability. One major obstacle is the difficulty of analysing complex, real-life samples in a cost-effective manner. Actual samples often contain a wide array of chemical species and contaminants that interfere with analysis, reducing sensitivity and reproducibility. While combining SERS with techniques like chromatography can help, such approaches require sophisticated equipment and trained personnel, limiting their use in point-of-care settings and increasing costs. To address these issues, current research focuses on creating smart, sustainable enhancing substrates with additional practical functionalities. These include flexible substrates, and integrated separation-enhancement, calibration-enhancement-in-one, and regeneration-enhancement capabilities. However, even with these advancements, challenges remain in areas such as automated mass production and storage stability. The "cheapness" of substrates must take into account production, application, storage, and disposal costs, while stability should be assessed over months rather than days. Ultimately, the path forward lies in smart substrate engineering and the discovery of novel enhancing materials, such as semiconductors and plasmonic polymers that offer comparable signal enhancement to traditional materials like gold and silver but at a lower cost. Standardized procedures for assessing substrate performance and applying SERS in

real-world scenarios are also crucial for broader adoption by non-specialist users. These combined efforts will pave the way for more sustainable and widespread SERS applications.[2]

This dissertation thesis began with a seed of curiosity, driven by the fact that the chemical enhancement method theory for Surface-Enhanced Raman scattering (SERS) is still not fully understood in some cases. The hypothesis is that if a nanoparticle is synthesized with an outer shell maintaining the distance of approximately 10 nm between the nanoparticle and an analyte molecule, surface-enhanced fluorescence could occur. However, achieving this specific distance is very difficult and requires complex processes.[3] In a fast-paced world, this study proposes to take a step back and revisit the fundamental processes of fluorescence and SERS, in the hope of contributing deeper insights into chemical enhancement.

The focus of this study is on the fundamental effects and interactions between a metal nanostructure and an analyte. The experiments were designed with the aim of uncovering additional information about these interactions and were carried out with curiosity, as this field of chemical enhancement in SERS still presents many unanswered questions. Our findings are based on SERS theory, various metal nanostructures, and two fluorophores, one positive and one negative. The importance of this subject lies in the need to develop more sensitive and accurate biosensors capable of tracking critical biomarkers associated with serious diseases. In this sense, the preliminary results from this study could pave the way toward more advanced biosensor development for the future of medicine, aiming for non-invasive, fast detection methods.

The first chapter focuses on the theoretical background necessary to conduct the experiments, offering a detailed description of fundamentals principles of SERS, the two complementary enhancement theories, and the role of biosensors in nanomedicine using fluroescence.

The second chapter presents an overview of the materials and methods used, beginning with the UV-Vis spectra of all silver nanostructures. It includes SERS and fluorescence experiments on the H_2O_2-AgNPs systems, which served as the first trial for achieving both fluorescence enhancement and quenching, using two fluorophores.

The final chapter introduces other silver nanostructures. The role and influence of the surfactant were studied in the presence of two fluorophores Alizarin Yellow and Nile Blue chloride under different conditions. The results of these tests support our hypothesis, highlighting the significance of surfactant-nanostructure interactions in enhancing or quenching fluorescence.

Chapter I: Theoretical concept

I.1 Nanotechnology and nanoscience

The last four decades have offered the medical field multiple discoveries based on interdisciplinarity. The collaboration between biology, chemistry, physics, and engineering has now led to nano-biotechnology, which is the base for disease diagnosis, drug delivery, and treatments. Nanotechnology has developed so much in recent years that it has the opportunity to provide the world with essential resources for healthcare diagnostics. Key parameters such as accuracy, sensitivity, and test reliability have been significantly improved by integrating nanoparticles with advanced imaging modalities, including magnetic resonance imaging (MRI), computerized tomography (CT) scans, and positron emission tomography (PET). [4] These hybrid techniques enable earlier and more accurate detection of pathological conditions, thereby improving clinical outcomes.

Driven by the need for more effective and non-invasive treatments, researchers continue to explore novel therapeutic strategies. Nanomedicine, a major outcome of nanotechnological research, has become an area of intense focus. By providing a deeper understanding of physiological and pathological processes at molecular level, nanotechnology enables the development of personalized and targeted medical interventions. The vast variety of domains nanostructures are used in, demonstrates the multiple purposes they can have in significant healthcare areas, including cancer therapy, gene therapy and diagnosis, for example. [5]

Biosensors in nanomedicine

Accurate disease detection is essential for applying the appropriate treatment. Biosensors represent a promising complement to conventional screening methods, particularly for the early detection of diseases. The key to simple and rapid diagnostics lies in the use of multifunctional, biocompatible, and non-invasive biosensors.

Recent advancements in this field are promising, as biosensors are increasingly being integrated into routine diagnostic procedures for the early detection of serious illnesses. Among their most important advantages are their low production cost and portability. Additionally, biosensors typically do not require high-power equipment and can be designed so that their effective detection area exceeds their physical dimensions.

These key features are largely dependent on the properties of the nanostructures used. Devices based on nanomaterials leverage the enhancement capabilities of metallic nanostructures,

combined with receptor-mediated detection and signal transduction. Together, these elements enable biosensors to function as point-of-care diagnostic tools and platforms for multiplexed monitoring. [6]

Biosensors based on nanostructures and fluorescence

The primary goals of a biosensor are to achieve high detectability, rapid response, non-invasiveness, and biocompatibility—particularly non-toxicity. One effective approach to meet these criteria is to develop biosensors based on metallic nanostructures and fluorescence. Point-of-care testing (POCT) systems have gained significant attention in the medical field because, unlike traditional methods, they employ a wide range of fluorescent dyes. This enables the simultaneous detection of multiple analytes from a single sample, allowing for faster and more sensitive identification of various biomarkers.

Ideally, the detection of dangerous and potentially life-threatening infections should be as simple and cost-effective as possible. POCT systems are designed with this in mind, incorporating key attributes such as high sensitivity, user-friendliness, speed, and specificity. According to existing research, the most common—though not exclusive—mechanisms for signal generation in biosensors include electrochemical detection, Raman scattering, magnetic sensing, surface plasmon resonance (SPR), and fluorescence-based techniques. Among these, the use of nanoparticles is particularly valuable for enhancing the fluorescent signal, thereby improving overall sensitivity and performance. [7]

I.2 Metal nanoparticles upbringing

The history of metal nanoparticles dates way back, from the time of other evolved civilisations. Whether it was gold or silver, people quickly discovered their properties and found clever ways to use them in various domains. For example, mineralogists in Egipt developed methods to purify the mined gold, therefore the objects from that period of time are evidence for the early use of this precious metal. A very important thing to mention when there is a talk about the history of gold nanoparticles is to mention the work of the alchemists. They used it for its medicinal values but also it was thought to be ”indestructible”. Apart from gold, silver was also very common in the precious metals domain and some researchers were brave enough to state that it was even more valuable than gold, as it was associated with purity and femininity. Objects fabricated with silver were also very precious because it also was called ”the white gold”. From a more recent perspective, metallic nanoparticles were studied by famous physicists and chemists

such as Michael Faraday and the optical properties they manifested were finally correlated to the different size possible of the nanoparticles. [8]

I.3 Properties of silver nanoparticles

The rapid expansion of the nanotechnology domain earned interest in the last decades, making almost every area of medicine, tratment and diagnosis include it. Because of its versatility, this new wave of nanomedicine makes a better option in comparison with existing techniques. What is so special about these metal-based nanoparticles? By changing different elements or quantities in the synthesis process, their qualities can change, serving specific properties. Various applications arise from this specific customization, for example, electronics, sensors, mechanics, chemistry, cosmetics, medicine and many more. Another important aspect for implementing nanoparticles is that their production process is customizable, cost-effective and environmentally friendly. Silver nanoparticles have a series of properties that make them very useful. A first one is their size, which can range from 1 nm to 100 nm. Even in simple conditions, the methods are widely used to produce efficient nanoparticles. The chemical process is based on using a reducing agent on silver ions and water of organic solvents until a colloidal dispersion occurs. The properties that set metallic nanoparticles apart from other materials are the physical, chemical and optical ones, making them a perfect candidate for biomedical applications. The key factors that hold the most importance over the characteristics of metallic nanoparticles are the surfactants, temperature, dispersing agents that influence the size, pH, time, pressure, and concentration of silver ion solution that influence their stability. [9]

I.4 Surface Enhanced Raman spectroscopy (SERS)

Raman spectroscopy, a vibrational spectroscopic technique, was first discovered in 1928 by C.V. Raman, describing the inelastic scattering of photons by molecules. In this process, photons interact with a molecular system, leading to a change in the molecule's vibrational, rotational, or electronic energy levels. The technique relies on the change in polarizability of a molecule during vibration, making it complementary to infrared (IR) spectroscopy, which depends on changes in the dipole moment. However, Raman spectroscopy suffers from low sensitivity, with only about one in 108 photons inelastically scattered. To overcome this limitation, Surface-enhanced Raman spectroscopy (SERS) was developed, significantly enhancing Raman signals for molecules near metallic nanostructures. SERS relies on the excitation of surface plasmon polaritons, creating intense electromagnetic fields that amplify Raman scattering.

The electromagnetic enhancement, the primary contributor to SERS, can increase signals by 4 to 8 orders of magnitude.

Chemical enhancement mechanisms also play a role, involving molecule-metal interactions and charge transfer processes, albeit to a lesser extent. SERS spectra can differ from traditional Raman spectra due to surface selection rules, where vibrational modes perpendicular to the metallic surface are enhanced. This high sensitivity and unique spectral characteristics have made SERS a powerful tool in various fields, including bioanalytics. [10]

While both localized surface plasmon resonance (LSPR) and surface-enhanced Raman spectroscopy (SERS) offer promising avenues for clinical applications, their limitations affect overall effectiveness. LSPR faces challenges related to its sensitivity to nanoparticle size, shape, and aggregation state, which can lead to variability in results. Achieving uniformity in complex nanostructures such as nanostars and nanoflowers, known for their tunable LSPR peaks, is particularly difficult, as these structures are prone to aggregation, compromising signal reliability. Similarly, nanorods and nanostars, despite offering tunable optical properties, present synthesis and control challenges, and also tend to aggregate, leading to inconsistent signals. SERS, while highly sensitive, encounters difficulties in quantitative analysis due to sensitivity to local optical fields at plasmonic hotspots within metallo-dielectric nanostructures. Variability in SERS substrates, caused by uneven distribution of localized electromagnetic fields across different plasmonic nanostructures, limits their suitability for routine quantitative applications.

Additionally, real-world samples often contain interfering substances that reduce Raman enhancement, making performance less reliable than in controlled laboratory environments. Furthermore, some publications claiming applicability in real-world environmental situations often find reduced Raman enhancement in complex matrices with interferences compared to straightforward laboratory samples. Despite these limitations, ongoing research aims to enhance the specificity, sensitivity, and reproducibility of both LSPR and SERS-based techniques, paving the way for their broader adoption in clinical diagnostics and monitoring.[11]

The electromagnetic (EM) enhancement theory

SERS relies heavily on the electromagnetic theory, which explains signal enhancement as a two-step process: local field enhancement and radiation enhancement. Local field enhancement occurs due to the excitation of localized surface plasmon resonances (LSPR) in metallic nanostructures. When light interacts with these nanostructures, energy is concentrated at nanoscale features such as edges and gaps, boosting the local electric field intensity by orders of magnitude. This enhanced field then interacts with nearby molecules, producing a stronger oscillating dipole at the Raman scattering frequency.

The second part, radiation enhancement, involves the amplification of the Raman-scattered fields. The EM field near a plasmonic nanostructured material is typically non-uniformly distributed, and often highly localized in spatially narrow regions, known as **SERS hotspots**. The overall SERS enhancement is the product of the incident and Raman enhancement processes . The total power at the Raman-scattered frequency is dissipated through radiation into the far-field (radiative power) and as heat in the plasmonic nanostructures (non-radiative power). While EM enhancement is the dominant mechanism, chemical enhancement also contributes to SERS. Chemical enhancement includes several phenomena such as ground-state interactions, resonance-like Raman processes and new resonances arising from photon-driven charge-transfer transitions. Unlike EM enhancement, which is primarily physical, chemical enhancement depends on the specific molecular states and the environment if the substrate surface. A unified theory of SERS would eventually merge both the EM and chemical aspects into a holistic quantum theory.[12]

Electromagnetic (EM) field concentrations play a crucial role in determining the effectiveness of SERS applications. Optimizing nanostructures for SERS involves maximizing the ability of plasmonic nanostructures to concentrate EM optical fields where molecules of interest are located. The intensity of the local EM field is significantly enhanced at nanoscale features, such as edges, tips, or crevices, due to the excitation of localized surface plasmons (LSPs). These areas of intense EM fields, are known as **hotspots** dramatically amplify Raman signals. The enhancement factor (EF) in SERS is often proportional to the fourth power of the electric field ($|E|^4$), indicating that even small increases in EM field concentration can lead to substantial improvements in SERS sensitivity. Multiscale EM coupling in hierarchical structures and hybridizing of antenna modes with a plasmonic waveguide cavity mode can further enhance the local field. The effectiveness of SERS is strongly influenced by the design and optimization of nanostructures capable of efficiently generating electromagnetic hotspots. Key factors such as the size, shape, material, and spatial

arrangement of the nanostructures determine the distribution of the electromagnetic field and, consequently, the magnitude of SERS enhancement. Overall, the ability to create and control EM field concentrations is central to maximizing the sensitivity and effectiveness of SERS in various applications, including trace-molecule detection, biomolecule analysis, and material characterization. [12]

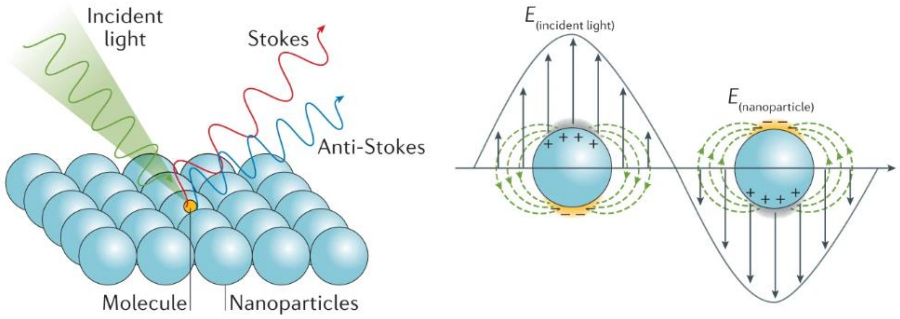

Fig. I-1. Schematic illustration of the EM effect in SERS [13]

Chemical enhancement mechanism theory

The chemical mechanism (CM) in SERS arises from the specific interactions between the molecule and the surface, playing a crucial role in determining the relative intensities of different Raman bands and providing insights into the local molecular environment. Unlike the electromagnetic mechanism (EM), the CM is directly related to the electronic structure of the molecule on the surface. It involves accounting for the wave function overlap between the molecule and the surface, leading to a renormalization of molecular energy levels and the introduction of metal-molecule charge-transfer states. The CM is categorized into static chemical interactions (CHEM), charge-transfer resonance (CT), and molecular resonance Raman scattering (RRS). CHEM is a consequence of the renormalization of the molecular energy levels, resulting in an increased polarizability of the molecule. CT involves electronic transitions between the metal and the molecule, while RRS is due to the molecular electronic and geometric changes resulting from binding to the surface. The interplay between CT and EM highlights the difficulty in separating these mechanisms. Full quantum mechanical methods are required for a complete description of SERS, necessitating the development of more efficient methods and required for a complete description of SERS, necessitating the development of more efficient computational techniques and improved interpretation of results.[14]

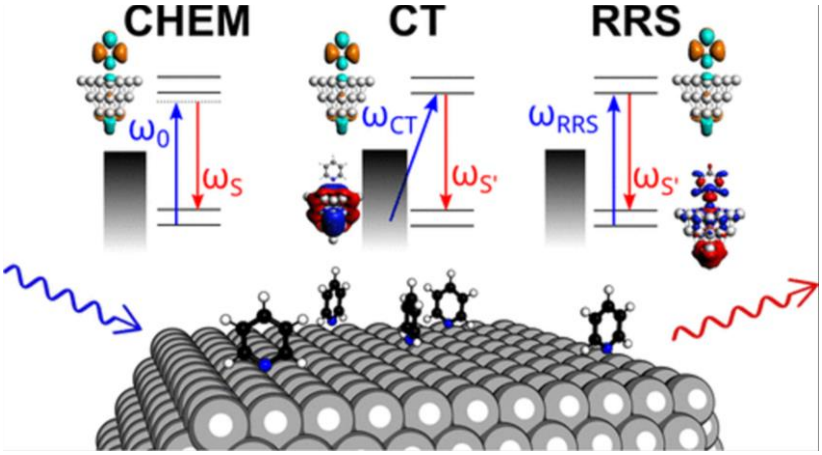

Fig. I-2 Chemical enhancement mechanisms in SERS [14]

Chapter II: Materials and Methods

II.1 Synthesis of silver nanoparticles with specific LSPR

The initial stage of this study involved the preparation of silver nanoparticle (AgNPs) solutions, synthesized through chemical reduction using sodium borohydride ($NaBH_4$) as the reducing agent, and stabilized with trisodium citrate dihydrate acting as a surfactant [15]. Colloidal silver nanoparticles with LSPR maxima at 390 nm, 520–530 nm, and 600–630 nm were obtained. These wavelengths were selected to partially overlap with the absorption bands of specific fluorophores employed in surface-enhanced fluorescence (SEF) studies and with the nanoparticle plasmon bands relevant for SERS, although not all correspond to the lasers intentionally used in order to test the correlation between the two types of spectroscopy. [16]

Silver nanoparticles were synthesized according to the procedure described by Zhang et al., which uses $NaBH_4$ as the reducing agent and sodium citrate as the surfactant. By varying the H_2O_2% concentration, nanostructures with different plasmonic bands were obtained. Using this synthesis method ensures that for all colloidal solutions, the nanoparticle surfaces are coated with the same molecule, thus avoiding interference from different surfactants in the adsorption of the target fluorophores. [17]

II.2 Silver nanoparticles characterization

These silver nanoparticles received the characteristics of tunable LSPR and, respectively, their colour by varying the quantity of hydrogen peroxide. So, considering this, the chosen colloids were the ones that exhibited LSPR at 393 nm, 510 nm, and 541 nm. For the yellow colloid with the absorption band at 393 nm, 40 µl of H_2O_2 was added. Following the same principle, for the indigo solution, 60 µl of H_2O_2 was added, and for the red one, 45 µl of H_2O_2 was used. It is noteworthy that the synthesis protocol is not entirely reproducible; however, for the purpose of this research, a single batch of colloid was sufficient to obtain the desired tunable LSPR properties.

Fig. II-1 Representative photograph of the H_2O_2-AgNPs

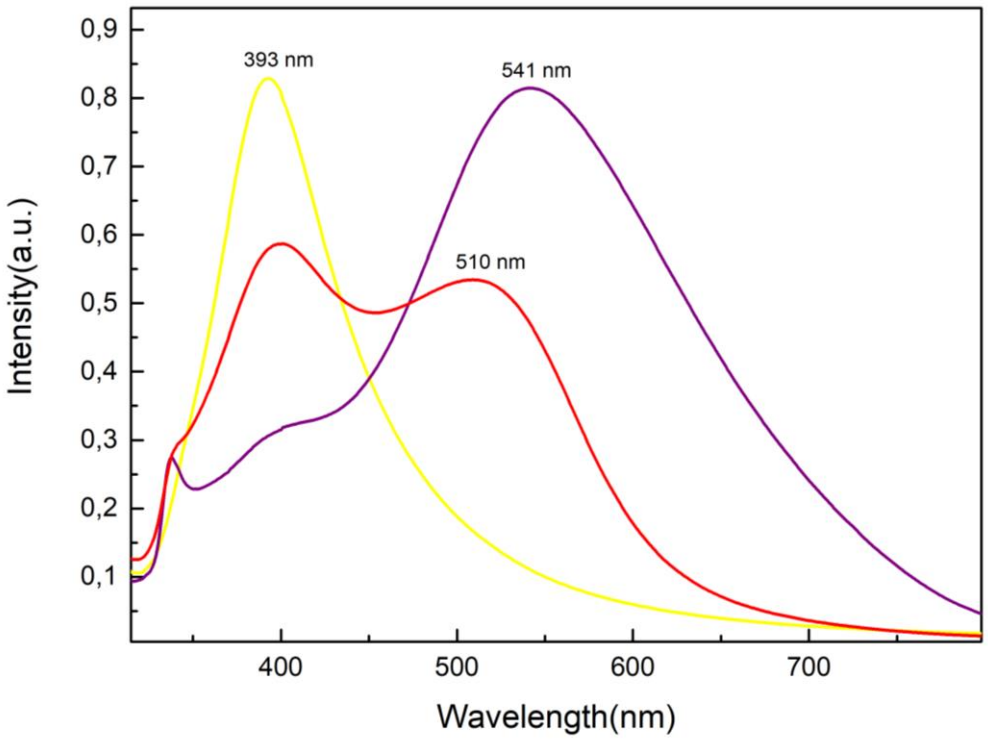

Fig. II-2 UV-Vis absorption spectra of H_2O_2-AgNPs synthesized with various H_2O_2 concentrations: 40 µl for yellow, 45 µl for red, 60 µl for indigo

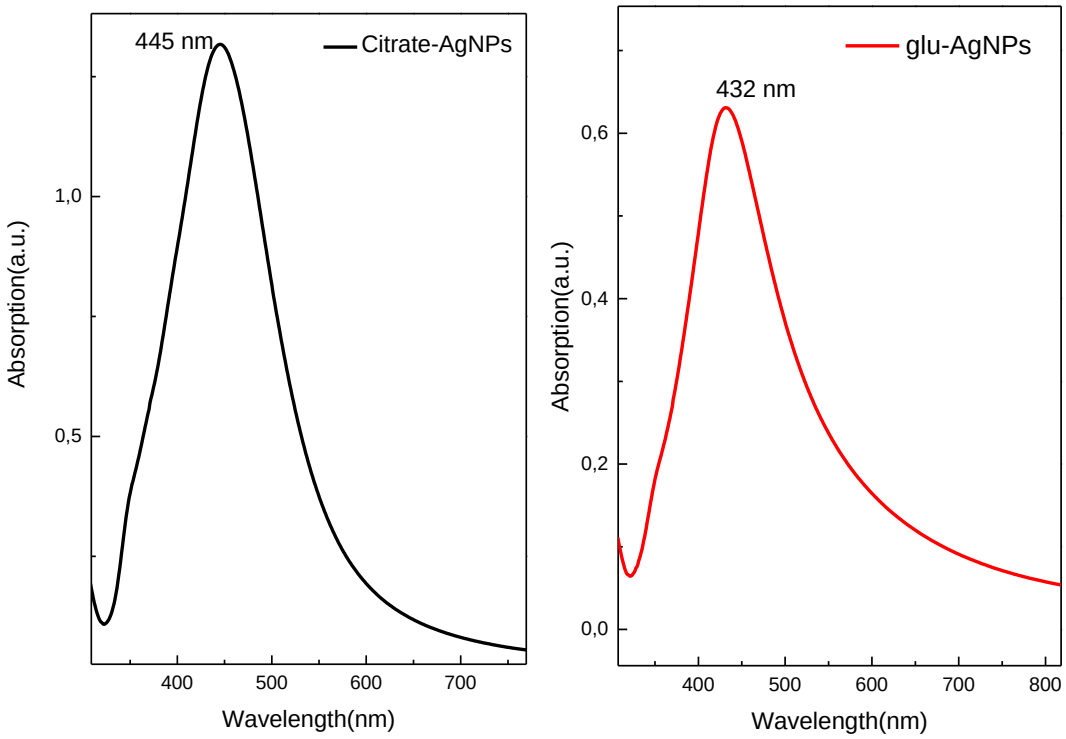

a) b)

Fig. II-3 UV-Vis absorption spectrum of: a) citrate-silver nanoparticles (cit-AgNPs), b) glucose-silver nanoparticles glu-AgNPs. SPR peaks are indicated in the figure.

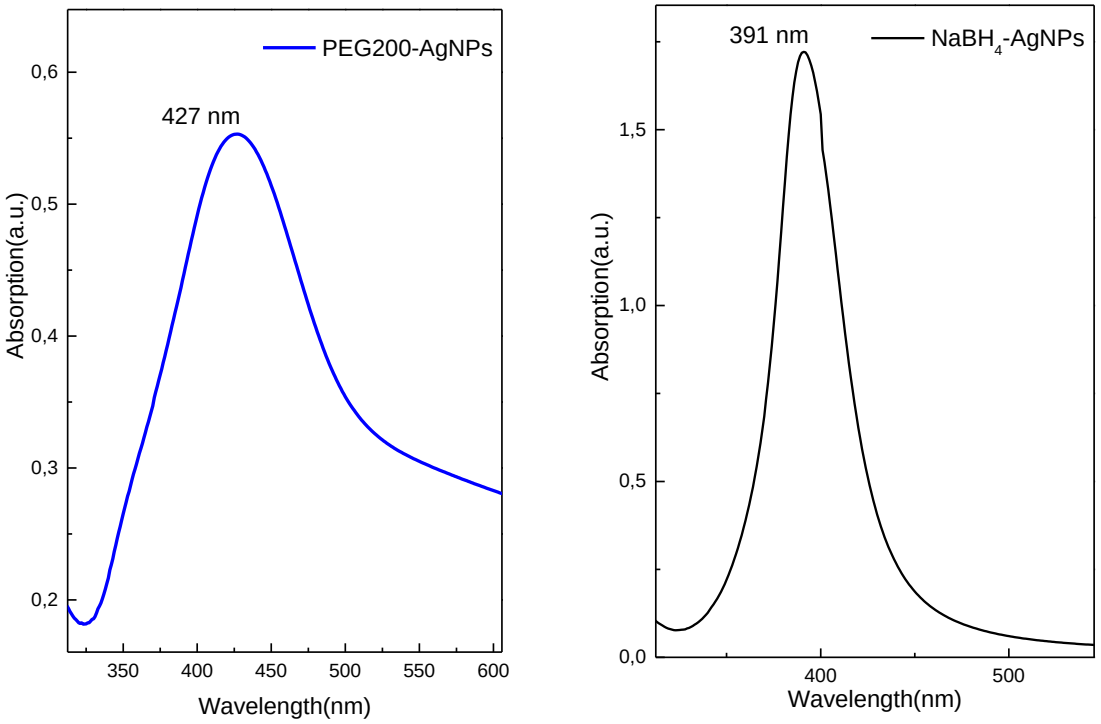

c) d)

Fig. II-4 UV-Vis absorption spectrum of c) PEG200-silver nanoparticles showing an SPR maximum at 447 nm,

and d) $NaBH_4$-silver nanoparticles showing an SPR maximum 391 nm

II.2.1 The significance of tunable LSPR and its applications

The remarkable properties of metal nanostructures observed in experiments have driven many researchers to explore the underlying theory of localized surface plasmon resonance (LSPR). The ability to tune LSPR has proven essential for a wide range of applications, prompting efforts to understand and control these phenomena at the nanoscale.

II.2.2 Fluorescence assays

A specific excitation wavelength is required for fluorescence to occur; therefore, a 630 nm LED was employed to match the absorption range of Nile Blue. The spectral analysis of silver nanoparticles with tunable LSPR, synthesized using H_2O_2 in the presence of Nile Blue, revealed that under certain wavelengths and experimental conditions, the fluorescence signal was significantly diminished. This observation suggests that Nile Blue molecules adsorb onto the nanoparticle surfaces, and that the spatial separation between the fluorophore and the nanoparticle surface is insufficient for surface-enhanced fluorescence (SEF), leading instead to fluorescence quenching.

This conclusion is supported by the observation that the fluorescence signal decreased by approximately half after mixing the fluorophore with the nanoparticles. It is plausible that, with an optimized ratio of colloid, dye, and ions, complete quenching could be achieved.

In the following spectra, it can be observed that there are two groups of peaks, one with higher intensity and the other with lower intensity. The more intense peak comes from the Nile Blue chloride molecules diluted in water at three different final concentrations: 10^{-6}M, $2x10^{-6}$M, and $4x10^{-6}$M. In the absence of silver nanoparticles, the addition of Ca^{2+} and Cl^- did not change the fluorescence signal much; they only decreased the intensity by a very small number of counts. In comparison, when the mix of Nile Blue chloride diluted in water with silver nanoparticles synthesized with H_2O_2, the intensity of fluorescence decreased significantly, even in the absence of positive or negative ions, approximately by half. The explanation is that the fluorophore molecules are adsorbed to the silver nanoparticles' surface, creating the quenching effect. Once again, by adding the ions, the fluorescence intensity slightly decreases, leading us to understand that more molecules are adsorbed to the nanoparticle surface, Cl^- attracting the positive molecules of Nile Blue chloride, and the Ca^{2+} holding them to the nanoparticle outer shell.

The band of interest for us is the one at approximately 675 nm that represents the emission domain of Nile Blue chloride.

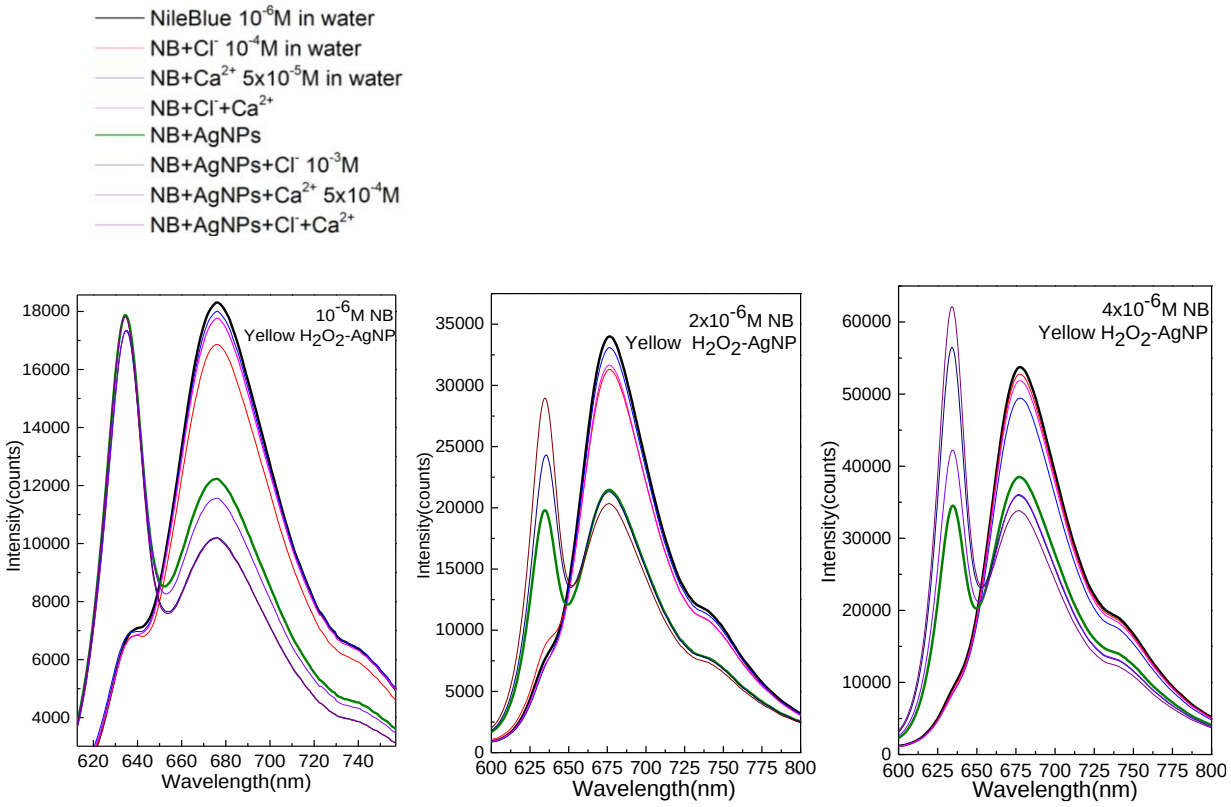

Fig. II-5 Fluorescence emission spectra of Nile Blue chloride diluted only in water (the more intense peak at ~ 675 nm) and with the yellow colloid (LSPR 393 nm) of lower intensity at different concentrations of NB: 10^{-6}M; $2x10^{-6}$M; $4x10^{-6}$M

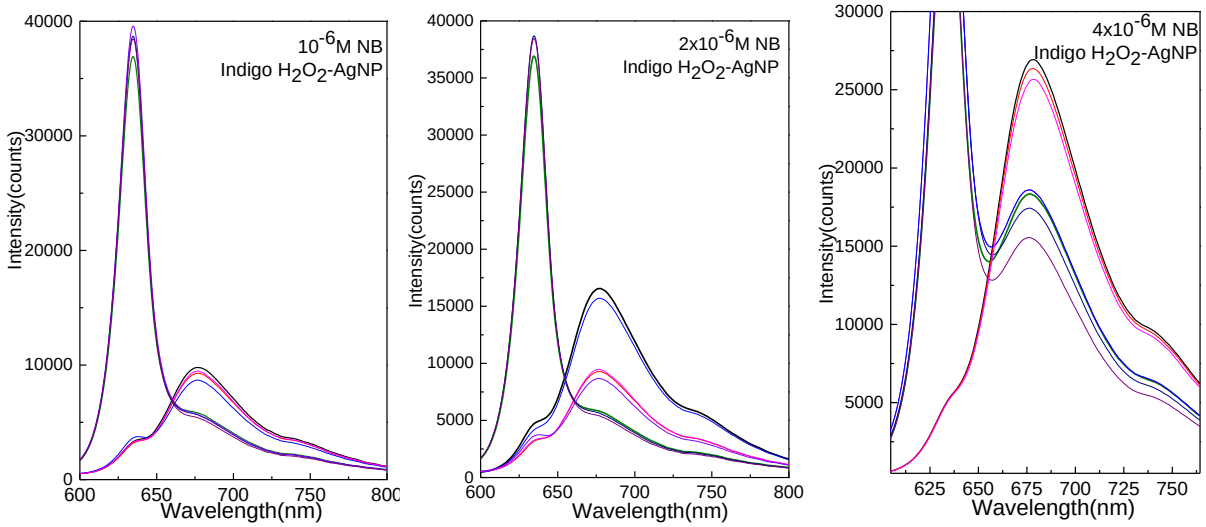

Fig. II-6 Fluorescence emission spectra of Nile Blue chloride diluted only in water (the more intense peak at ~ 675 nm) and with the indigo colloid (LSPR 541 nm) of lower intensity at different concentrations of NB: 10^{-6}M; $2x10^{-6}$M; $4x10^{-6}$M

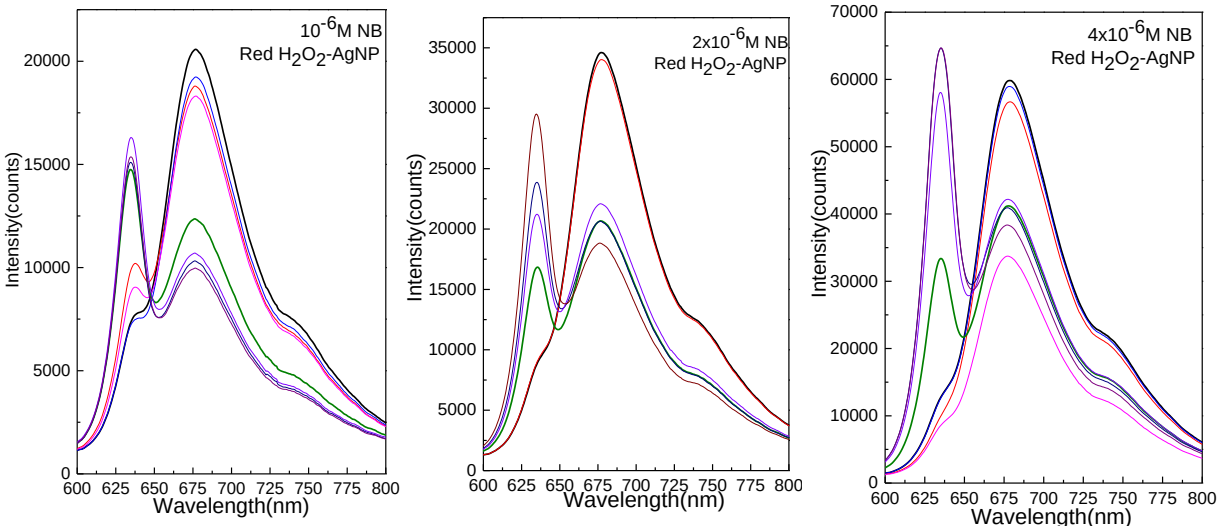

Fig. II-7 Fluorescence emission spectra of Nile Blue chloride diluted only in water (the more intense peak at ~ 675 nm) and with the yellow colloid (LSPR 510 nm) of lower intensity at different concentrations of NB: 10^{-6}M; $2x10^{-6}$M; $4x10^{-6}$M

The findings after this type of experiment were that, after mixing a colloid with a fluorophore, a part of the molecules will adsorb to the surface of the silver nanoparticles, turning the fluorescence signal down. In this case, the goal was to see how much the final molar concentration of the fluorophore would influence the fluorescence signal, without changing the one for the nanoparticles, and with some additional positive and negative ions.

II.2.3 SERS with yellow, indigo and red colloids

The test compound Nile Blue was added to citrate-stabilized silver nanoparticles (cit-AgNPs), and was examined using two LED excitation wavelengths: 532 nm and 633 nm. The results indicated that the yellow nanoparticle solution yielded superior SERS performance. Notably, upon the addition of 10^{-3} M chloride ions, the initially indigo or red solution immediately shifted to yellow, and only under these conditions did it exhibit strong SERS signals.

532_nm YELLOW INDIGO RED

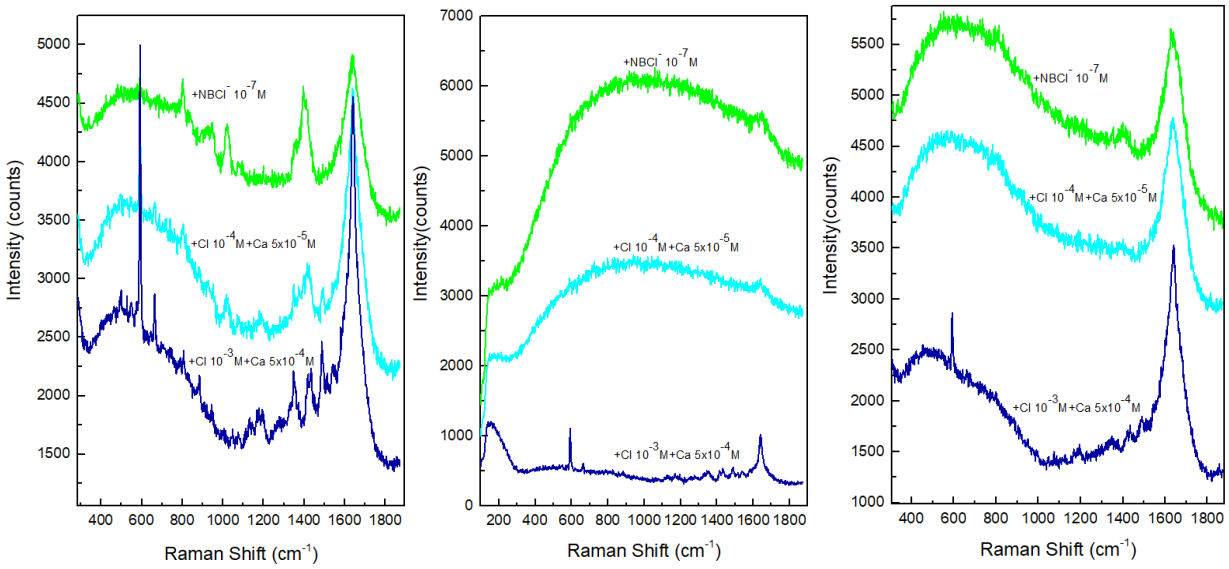

Fig. II-8. SERS spectra of Nile Blue following the addition of various concentrations of atomic ions to the silver colloidal solutions. Excitation wavelength: 532 nm.

633 nm YELLOW INDIGO RED

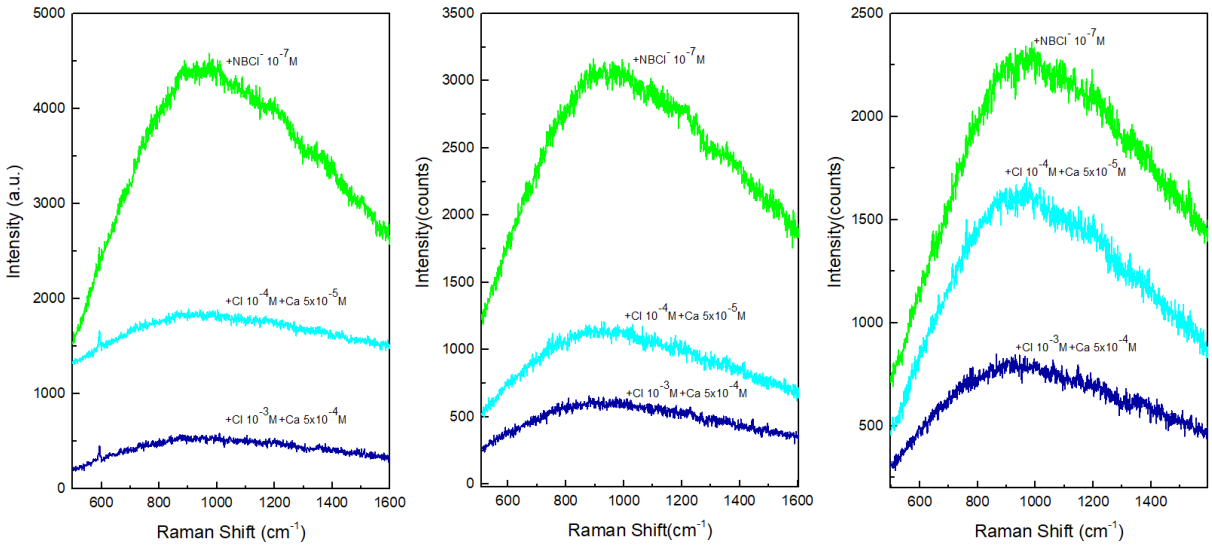

Fig. II-9. SERS spectra of Nile Blue following the addition of various concentrations of atomic ions (Cl^- 10^{-4}M+Ca^{2+} 10^{-5}M and Cl^- 10^{-3}M+ Ca^{2+} 10^{-4}M) to the silver colloidal solutions. Excitation wavelength: 633 nm

The signal decreased upon the addition of negative ions, while the presence of positive ions led to a reduction in fluorescence intensity. Interestingly, the combination of both ion types enhanced the overall SERS signal under 532 nm laser excitation (Fig. II-8).

However, this enhancement was not observed under 633 nm excitation. Since the absorption window of Nile Blue includes the 630 nm region, the resonance at this wavelength was excessively strong. As a result, the spectrum in Fig. II-9 is dominated by fluorescence emission from the analyte, with a minimal detectable Raman signal

Chapter III: Surfactant importance

III.1 SERS of silver nanostructures with different surfactants

As is well known, every molecule exhibits a unique vibrational signature—its molecular "fingerprint"—which enables the precise identification of substances within a mixture. But what if we want to test the selectivity of a silver nanostructure? Under specific conditions, selectivity can indeed be achieved, with the surfactant used during synthesis playing a crucial role in guiding this process.

Limit of detection

To determine the optimal concentrations for each type of surfactant, the first step was to assess their performance. By increasing the concentration of the fluorophore, there is also an evolution of the SERS signal, but the most important part was the right amount of molecules to make it appear. The gradual increase in intensity of the SERS spectra was due to the addition of a larger number of fluorophore molecules, also increasing the odds of adsorption on the nanoparticle surface.

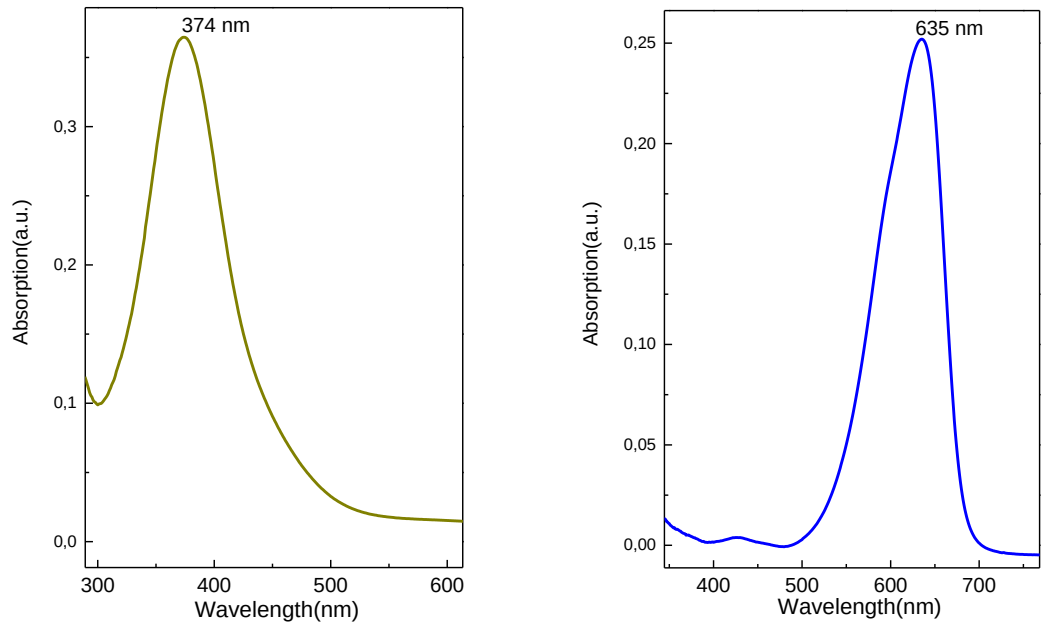

a) b)

Fig. III-1 UV Vis absorption spectra of a) Alizarin Yellow; b) Nile Blue in water

The absorbance range of a fluorophore carries the same importance as the colloid one, because they need to overlap in order to meet the expectations of the hypothesis.

Alizarin Yellow R

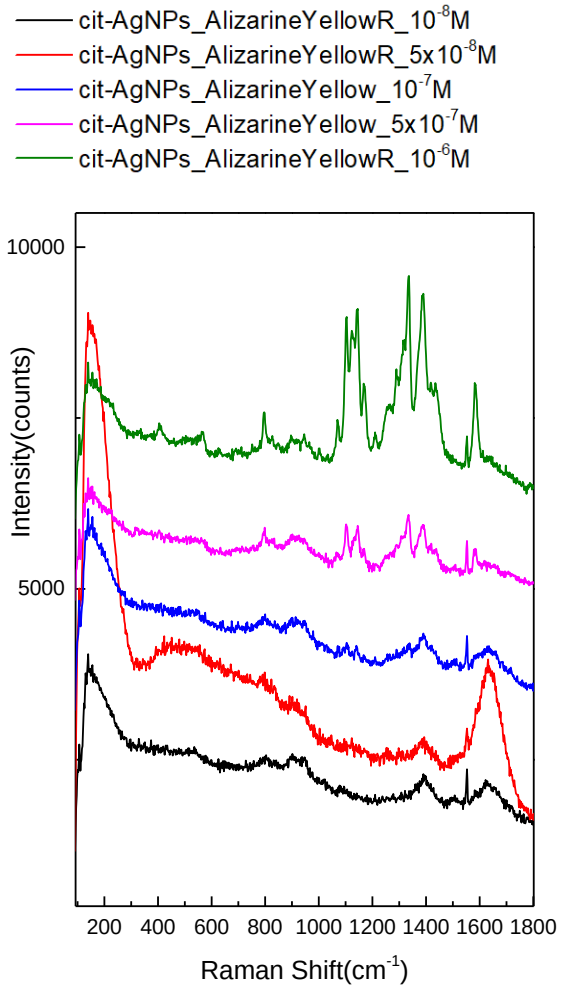

Fig. III-2. SERS spectra of Alizarin Yellow at the indicated concentrations, using silver nanoparticles synthesized via citrate reduction (citrate as surfactant).

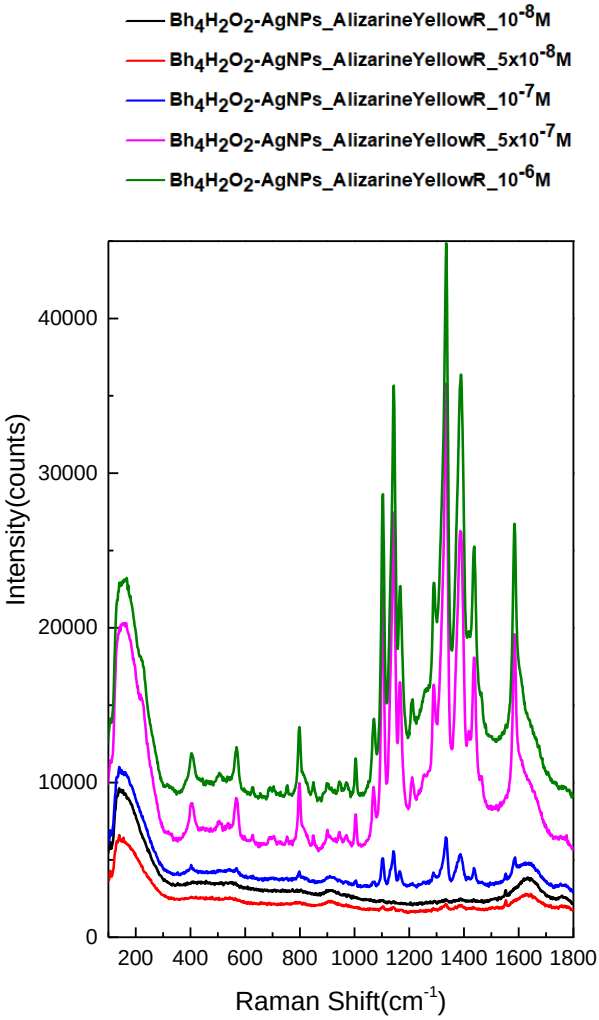

Fig. III-3 SERS spectra of Alizarin Yellow at the indicated concentrations, using silver nanoparticles synthesized via borohydride reduction (boric acid as surfactant).

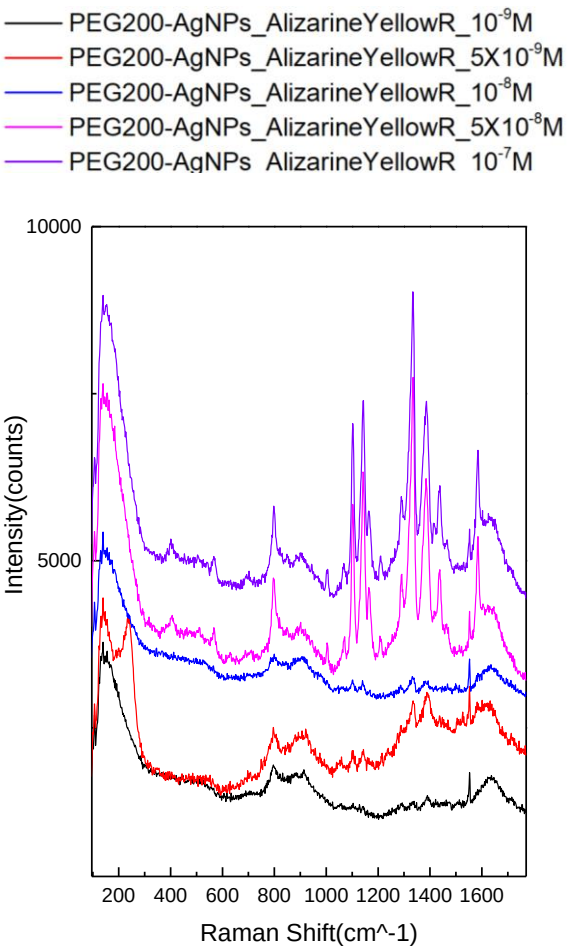

Fig. III-4. SERS spectra of Alizarin Yellow at the indicated concentrations, using silver nanoparticles synthesized via PEG200 reduction (PEG200 as surfactant).

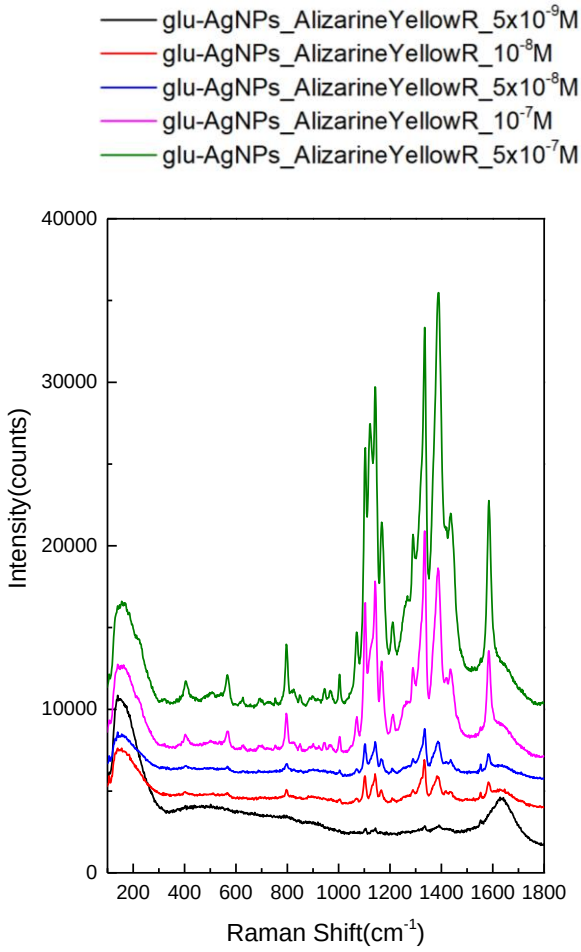

Fig. III-5 SERS spectra of Alizarin Yellow at the indicated concentrations, using silver nanoparticles synthesized via glucose reduction (glucose as surfactant).

Similarly, Nile Blue was also evaluated for its detection potential. However, detecting Nile Blue proved to be more challenging, prompting the addition of anionic and cationic species to enhance.

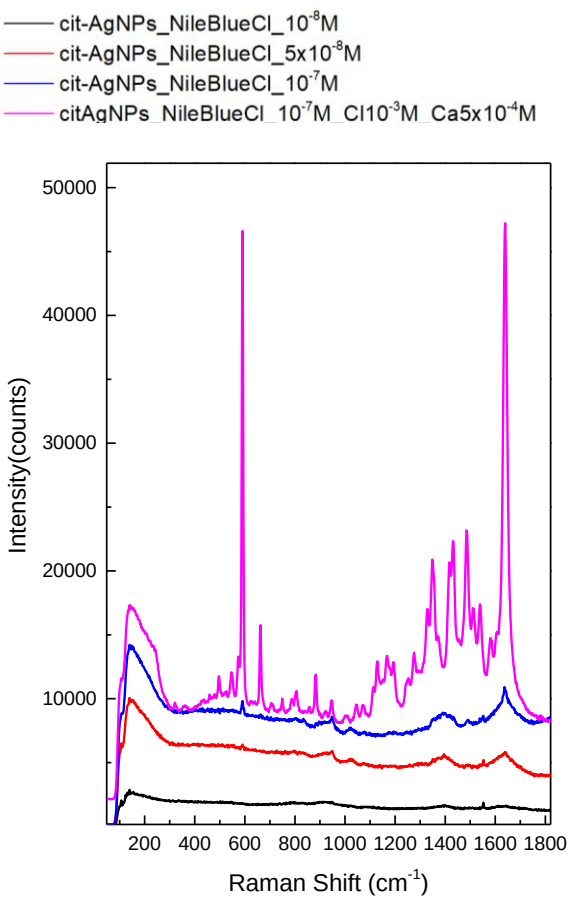

Fig. III-6. SERS spectra of Nile Blue at the indicated concentrations and atomic ions supplementation, using silver nanoparticles synthesized via citrate reduction (citrate as surfactant).

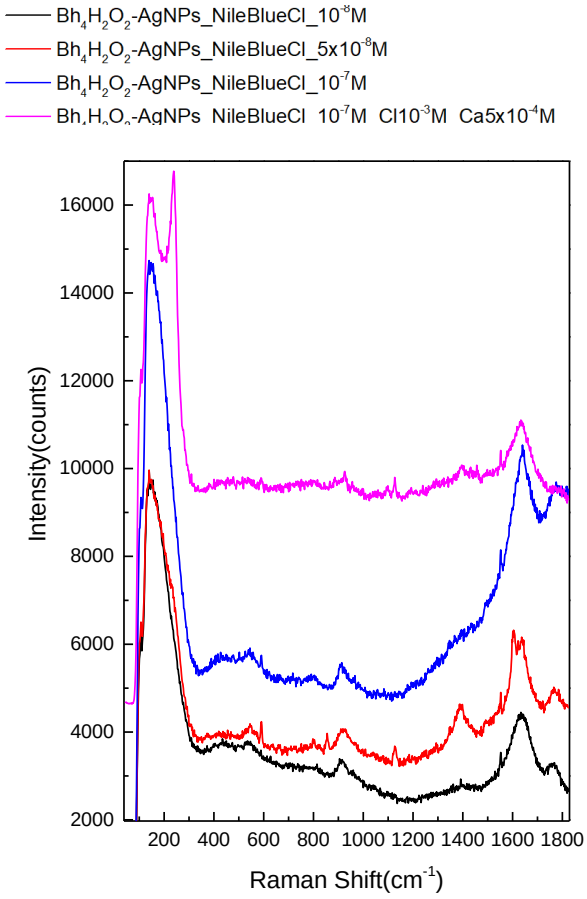

Fig. III-7. SERS spectra of Nile Blue at the indicated concentrations and atomic ions supplementation, using silver nanoparticles synthesized via borohydride reduction (boric acid as surfactant).

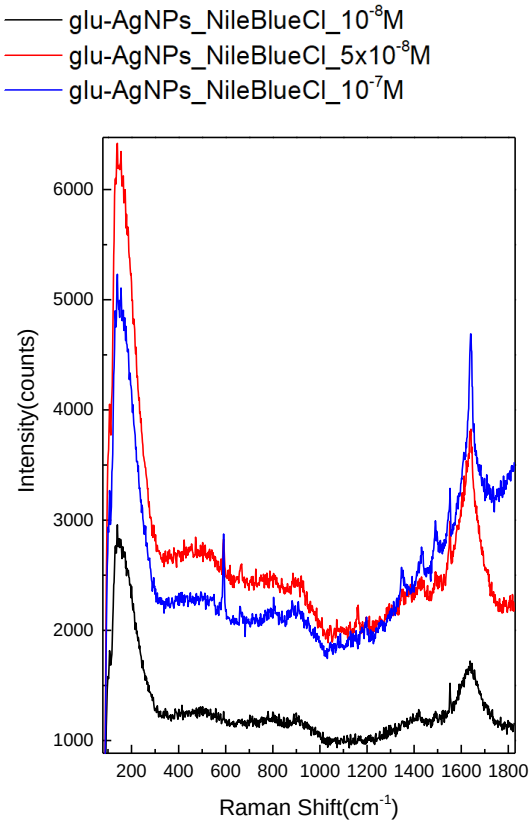

Fig. III-8. SERS spectra of Nile Blue at the indicated concentrations and atomic ions supplementation, using silver nanoparticles synthesized via glucose reduction (glucose as surfactant).

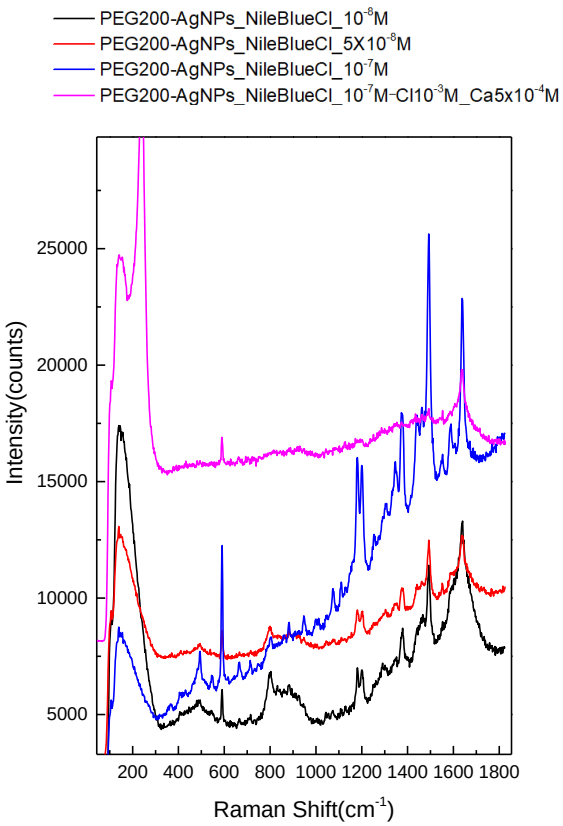

Fig. III-9. SERS spectra of Nile Blue at the indicated concentrations and atomic ions supplementation, using silver nanoparticles synthesized via PEG200 reduction (PEG200 as surfactant).

Increasing the analyte concentration leads to a stronger SERS signal, as more analyte molecules become available for adsorption onto the surface of the silver nanostructures. The primary objective is to assess the variation in SERS performance among nanoparticles synthesized using different surfactants and to determine whether a correlation exists between the type of surfactant and the resulting SERS signal. To better understand this relationship, a comparative analysis will be carried out using silver nanostructures prepared with various surfactants, while maintaining a constant final molar concentration of the analytes.

The following example clearly illustrates the differences between various colloids and highlights the influence of surfactants in the absence of additional positive or negative ions. Among the tested systems, the colloid stabilized with glucose as a surfactant yielded the strongest SERS signal. This is likely due to the ease with which glucose molecules can be displaced from the nanoparticle surface, allowing the fluorophore to adsorb more effectively.

Based on this principle of surface affinity, when maintaining a constant final analyte concentration of 10^{-7} M for both Nile Blue and Alizarin Yellow, each colloid exhibited different detection limits, as shown in Figures III-10 and III-11. These variations reflect the influence of surfactant type on molecule–nanoparticle interactions.

A direct comparison of the two fluorophores at the same concentration (10^{-7} M), across nanoparticles synthesized with different surfactants and supplemented with Ca^{2+} and Cl^{-} ions, reveals key differences in adsorption behavior. By altering the nanoparticle's outer layer through surfactant selection, the adsorption efficiency of analyte molecules—whether cationic or anionic—changes accordingly. Figure III-10 illustrates the interaction of Alizarin Yellow R (an anionic molecule), while Figure III-11 depicts that of Nile Blue (a cationic molecule), with the surrounding nanoparticle layer.

The affinity of the nanoparticle surface plays a crucial role in determining which molecules can effectively adsorb. As demonstrated, glucose-stabilized nanoparticles allowed the easiest replacement of the surfactant, enabling strong interaction between the fluorophore and the metal surface. With the assistance of calcium and chloride ions, the fluorophore successfully displaced the glucose molecules, resulting in a significantly enhanced SERS signal.

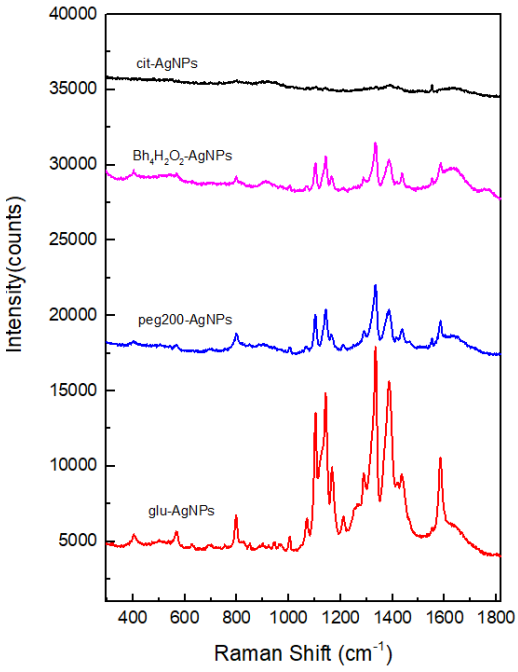

Fig. III-10. SERS spectra of Alizarin Yellow using the indicated colloidal solutions as substrate.

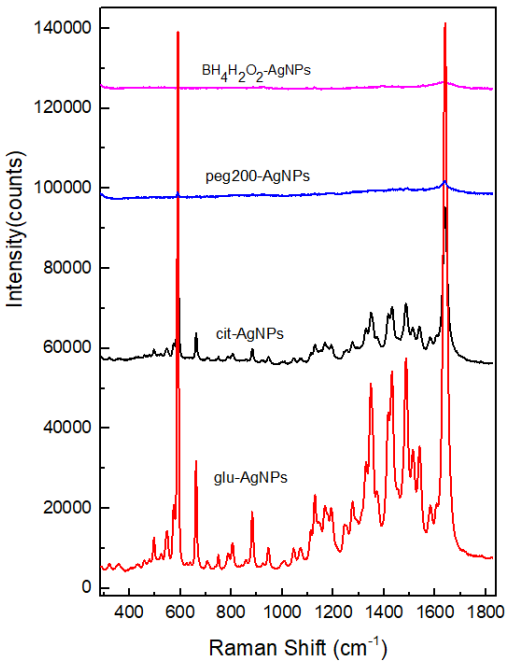

Fig. III-11. SERS spectra of Nile Blue using the indicated colloidal solutions as substrate.

Surfactant-dependent selectivity for anionic and cationic fluorophores

Following the series of experiments involving various colloids, fluorophores, and both anionic and cationic molecules, the question of selectivity naturally arose. To explore this, a mixed solution containing citrate-stabilized and PEG200-stabilized colloids was prepared, along with Alizarin Yellow (with Ca^{2+}) and Nile Blue (with Ca^{2+} and Cl^{-}), and tested under laser excitations at 532 nm and 633 nm. The resulting spectra revealed a clear distinction between the signals of Alizarin Yellow and Nile Blue, confirming that, with appropriate conditions and molecular interactions, it is indeed possible to selectively detect specific molecules within a complex mixture.

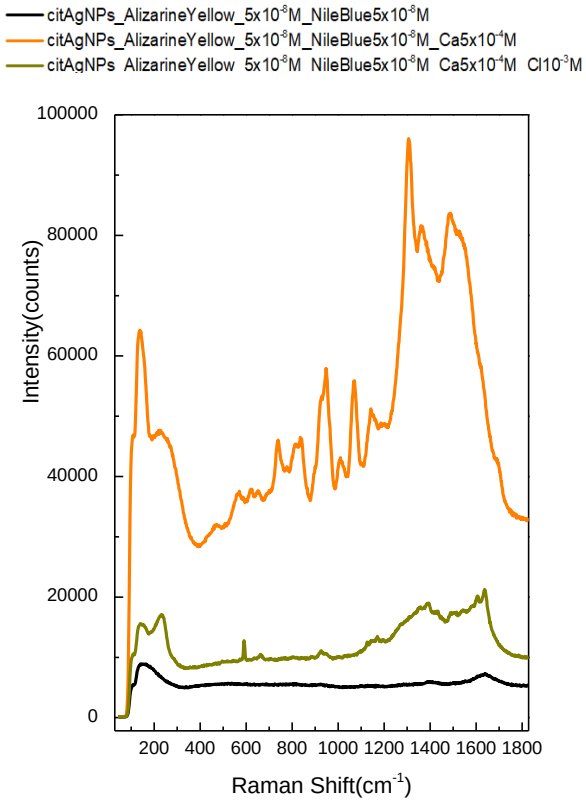

a)

Fig. III-12. SERS spectra of a mixture of Alizarin Yellow and Nile Blue at the indicated concentrations were recorded using citrate-reduced colloidal silver nanoparticles and 532 nm laser excitation. The spectral table summarizes the optimal conditions for enhancing the SERS signal of each dye.

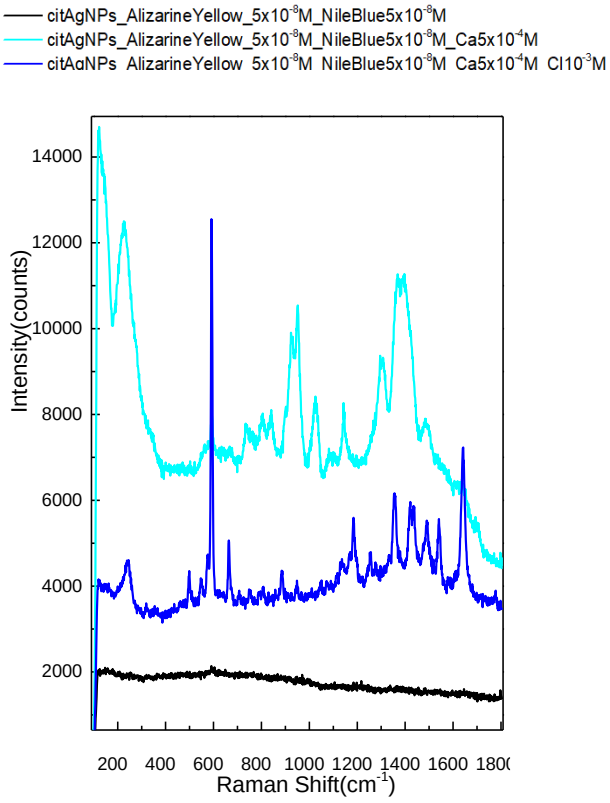

b)

Fig. III-13. SERS spectra of a mixture of Alizarin Yellow and Nile Blue at the indicated concentrations were recorded using citrate-reduced colloidal silver nanoparticles and 633 nm laser excitation. The spectral table summarizes the optimal conditions for enhancing the SERS signal of each dye.

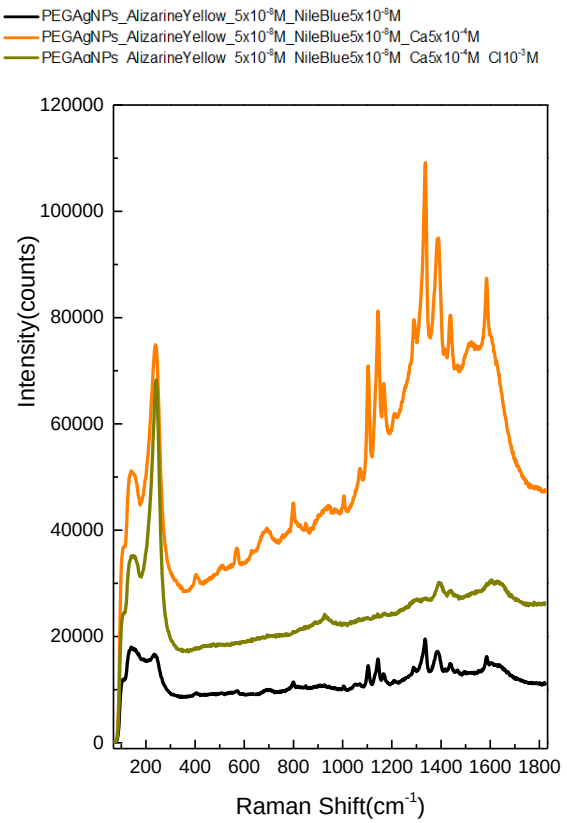

c)

Fig. III-14. SERS spectra of a mixture of Alizarin Yellow and Nile Blue at the indicated concentrations were recorded using PEG200-reduced colloidal silver nanoparticles and 532 nm laser excitation. The spectral table summarizes the optimal conditions for enhancing the SERS signal of each dye.

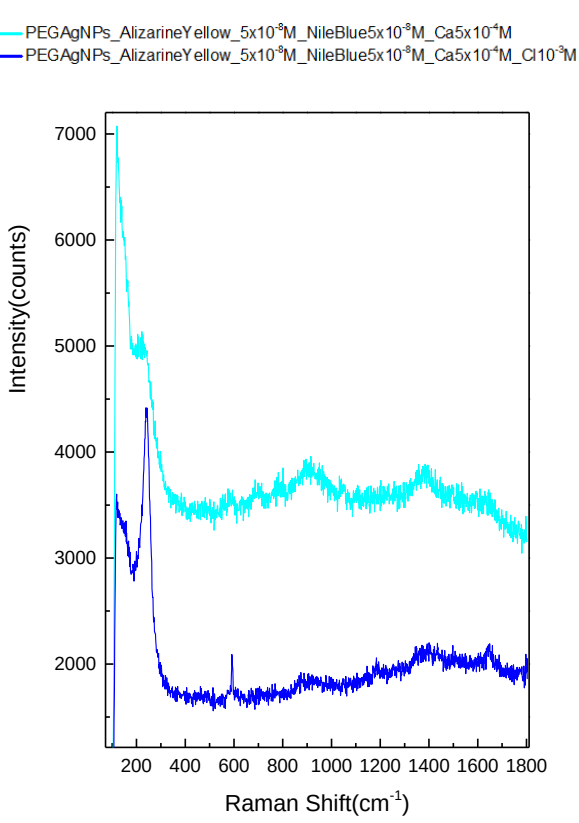

d)

Fig. III-15. SERS spectra of a mixture of Alizarin Yellow and Nile Blue at the indicated concentrations were recorded using PEG200-reduced colloidal silver nanoparticles and 633 nm laser excitation. The spectral table summarizes the optimal conditions for enhancing the SERS signal of each dye.

Notably, under 532 nm excitation, the addition of Cl^- ions to the dye mixture—conditions that would typically enhance the SERS signal of Alizarin Yellow—led instead to a suppression of its spectral features. The few peaks that appeared were weak and did not match the characteristic signature of Alizarin Yellow. A plausible explanation is that the presence of Cl^- ions favoured the adsorption or SERS enhancement of Nile Blue over Alizarin Yellow, resulting in a shift in the dominant spectral response.

III.2 The electrical charge of the silver nanoparticles

During the experiment, another critical aspect emerged regarding the surface properties of the silver nanoparticles. Specifically, the electrical charge and Fermi level of the nanoparticles were found to influence the adsorption behavior of surrounding molecules. To investigate this, various substances were added to both the colloid and the colloid-fluorophore mixtures to modulate the appearance or suppression of the SERS signal.

The adsorption of halide ions (Cl^-, Br^-, I^-) onto silver nanoparticles induces an upshift in the Fermi level of the plasmonic system, which significantly impacts charge transfer processes at the metal–molecule interface. Strong adsorption of these anions leads to a notable increase in the Fermi level of AgNPs, following the trend $Cl^- < Br^- < I^-$. This upshift promotes spontaneous electron transfer to molecular orbitals that are energetically aligned with the raised Fermi level, continuing until charge neutrality is achieved at the interface. [18]

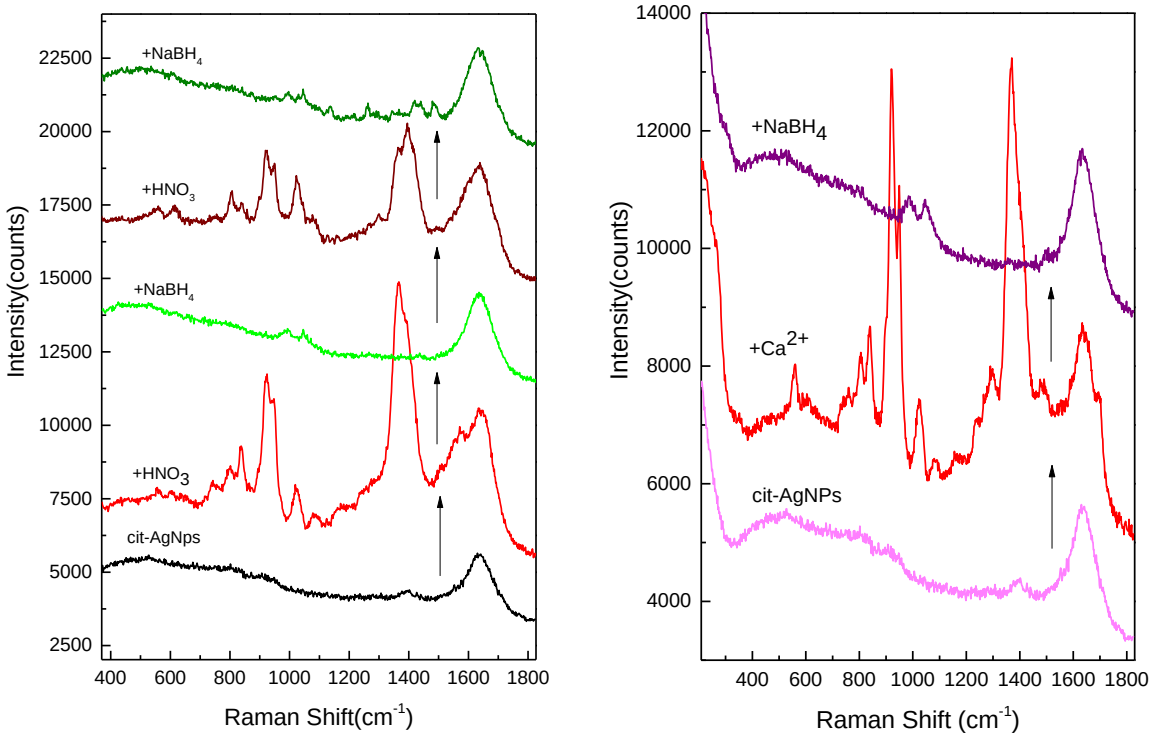

Figs. III-16. SERS spectra of cit-AgNPs in different conditions, as labelled.

These SERS spectra of citrate-capped silver nanoparticles (cit-AgNPs) demonstrate the ability to reversibly switch the citrate signal on and off, depending on the chemical equilibration of the silver surface with the surrounding medium. To activate the citrate SERS signal, nitric acid (HNO_3) was added, lowering the pH and inducing partial dissolution of the AgNP surface. This results in the formation of Ag^+ ions, which lowers the Fermi level of the nanoparticles.

The reduced Fermi level favors the adsorption of citrate onto the newly formed Ag^+ sites, leading to the appearance (turn-on) of the citrate SERS spectrum (Figure III-16A).

The citrate signal can be turned off by reducing these Ag^+ sites with sodium borohydride ($NaBH_4$), a strong reducing agent that donates electrons to the nanoparticle, thereby restoring metallic silver and increasing the Fermi level. This electron enrichment suppresses citrate adsorption, resulting in the disappearance (turn-off) of the citrate SERS signal. This process of Ag^+ site formation and subsequent reduction was repeated multiple times, clearly demonstrating the reversible switching of the citrate SERS spectrum. These findings highlight the critical role of analyte adsorption and Fermi level modulation in the activation of SERS signals.

Interestingly, a similar reversible behavior was observed when HNO_3 was replaced with calcium nitrate ($Ca(NO_3)_2$) (Figure III-16B). The addition of Ca^{2+} to cit-AgNPs also induced a turn-on of the citrate SERS signal. This is consistent with recent studies suggesting that Ca^{2+} lowers the Fermi level of AgNPs, possibly by promoting the formation of Ag^+. Upon subsequent addition of $NaBH_4$, the citrate signal was again suppressed, supporting the hypothesis that Ca^{2+}-induced enhancement is also linked to Ag^+ formation, which can be reversed by reduction.

Next, we explored the role of Ag^+ formation and chemical equilibration in the SERS behavior of a cationic molecule, Nile Blue (Figure III-17).

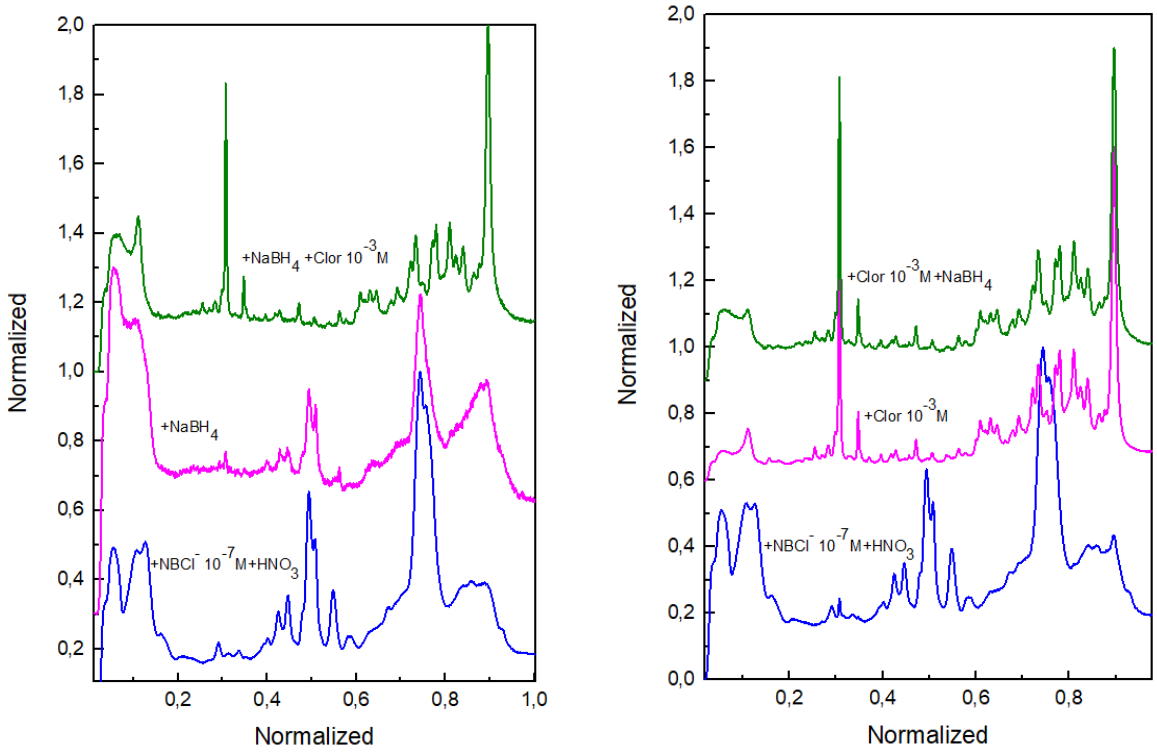

Figs. III-17. SERS spectra of Nile Blue recorded using citrate-capped silver nanoparticles (cit-AgNPs) as the substrate, with various added species as indicated.

The partial dissolution of AgNPs results in the appearance of the SERS spectrum of citrate, the nanoparticle capping agent. A weak SERS band of Nile Blue also emerges at 590 cm^{-1}. However, reduction of Ag^{+} to Ag^{0} using $NaBH_4$ did not trigger a turn-on of the Nile Blue SERS signal. Sequential addition of Cl^{-} ions, on the other hand, led to the appearance of distinct SERS bands for Nile Blue, accompanied by a weak band at 240 cm^{-1}, corresponding to Ag–Cl formation.

Interestingly, when Cl^{-} was added immediately after the formation of Ag^{+} sites, a much stronger SERS signal of Nile Blue was observed, along with a pronounced Ag–Cl band at 242 cm^{-1}. Subsequent addition of $NaBH_4$ did not significantly alter the Nile Blue SERS spectrum, although a decrease in the Ag–Cl band intensity was noted. This is likely due to the reduction of Ag^{+} back to Ag^{0} and the consequent desorption of Cl^{-} from the nanoparticle surface.

Conclusions

This study reinforces the versatility and potential of silver nanostructures in surface-enhanced Raman scattering (SERS) as powerful tools for probing surface interactions between nanoparticles and analytes. Initial performance assessments using H_2O_2-synthesized AgNPs revealed tunable localized surface plasmon resonance (LSPR), with favorable spectral alignment for both LED excitation and Nile Blue fluorescence—key parameters for dual-mode fluorescence and SERS applications. While the results were promising, they also highlight the need for further optimization and investigation. Notably, a strong SERS signal from Nile Blue was only observed following the addition of both cations and anions, accompanied by an immediate color change from indigo-red to yellow, indicating significant chemical and optical transformations.

The study also demonstrated selective molecular detection under specific conditions. For Alizarin Yellow R, a detection limit of 10^{-9} M was achieved using four different types of AgNPs synthesized with distinct surfactants—without requiring additional ionic enhancers. For Nile Blue, the detection limit was 10^{-8} M. Among the surfactants tested, glucose was found to enhance signal intensity. Selectivity was further confirmed by mixing Alizarin Yellow and Nile Blue with cit-AgNPs and PEG200-AgNPs. Under carefully controlled excitation conditions and ionic environments, the SERS spectra of the two dyes could be clearly differentiated.

Finally, the role of nanoparticle surface charge and electronic properties was explored. The presence of chemical species capable of modulating the Fermi level—either through electron donation or withdrawal—was shown to have a substantial effect on the SERS response. This emphasizes the critical importance of surface electronic structure in the detection and characterization of molecular species via SERS.

Annexes

Annex 1

UV-Vis Spectroscopy

In this study, silver nanoparticles were characterized in terms of their optical properties using a Jasco V-630 UV-Vis spectrophotometer. Measurements were performed in a quartz cuvette with a 1 nm optical path length, using distilled water as the reference. The instrument emits light in the ultraviolet and visible ranges, which is directed through a prism to disperse it into its component wavelengths. One beam is directed through the sample via a system of mirrors, while the other passes through the reference. The spectrophotometer then measures the difference in light intensity between the sample and reference paths, and the data are presented as absorbance or transmittance spectra as a function of wavelength

Fig. 1. UV-Vis spectrophotometer used in this study.

The primary objective of this analysis was to characterize the optical properties of various silver nanostructures synthesized through different methods, with the aim of obtaining multiple, tunable localized surface plasmon resonance (LSPR) peaks. These tunable LSPR features are essential for optimizing the interaction with different fluorophores in subsequent SERS investigations.

Renishaw inVia Raman Spectrometer

All SERS and Raman measurements in this study were conducted using the Renishaw inVia Raman spectrometer, a key instrument in this research. The system includes an integrated optical microscope, enabling real-time imaging and precise targeting of sample areas—an essential feature for accurate spectral acquisition. A significant advantage of this spectrometer is its capability for Raman mapping, allowing for spatially resolved analysis of chemical composition. Furthermore, the instrument is equipped with multiple laser lines, providing flexibility in excitation wavelength selection to optimize spectral resolution and signal enhancement based on the specific requirements of each experiment [20]

Fig. 2 Renishaw inVia Raman Spectrometer used in this study.

References

[1] M. Tavakkoli Yaraki, A. Tukova, și Y. Wang, „Emerging SERS biosensors for the analysis of cells and extracellular vesicles”, *Nanoscale*, vol. 14, nr. 41, pp. 15242–15268, 2022, doi: 10.1039/D2NR03005E.

[2] C. Li *et al.*, „Towards practical and sustainable SERS: a review of recent developments in the construction of multifunctional enhancing substrates”, *Journal of Materials Chemistry C*, vol. 9, nr. 35, pp. 11517–11552, 2021, doi: 10.1039/D1TC02134F.

[3] S. D. Catingan și A. Moores, „Recent Progress in Surface-Enhanced Fluorescence Using Gold Nanorods”, *ACS Appl. Nano Mater.*, vol. 7, nr. 16, pp. 18467–18485, aug. 2024, doi: 10.1021/acsanm.3c04756.

[4] S. Malik, K. Muhammad, și Y. Waheed, „Emerging Applications of Nanotechnology in Healthcare and Medicine”, *Molecules*, vol. 28, nr. 18, Art. nr. 18, ian. 2023, doi: 10.3390/molecules28186624.

[5] A. Haleem, M. Javaid, R. P. Singh, S. Rab, și R. Suman, „Applications of nanotechnology in medical field: a brief review”, *Global Health Journal*, vol. 7, nr. 2, pp. 70–77, iun. 2023, doi: 10.1016/j.glohj.2023.02.008.

[6] A. I. Barbosa, R. Rebelo, R. L. Reis, M. Bhattacharya, și V. M. Correlo, „Current nanotechnology advances in diagnostic biosensors”, *MEDICAL DEVICES & SENSORS*, vol. 4, nr. 1, p. e10156, 2021, doi: 10.1002/mds3.10156.

[7] D. Semeniak, D. F. Cruz, A. Chilkoti, și M. H. Mikkelsen, „Plasmonic Fluorescence Enhancement in Diagnostics for Clinical Tests at Point-of-Care: A Review of Recent Technologies”, *Advanced Materials*, vol. 35, nr. 34, p. 2107986, 2023, doi: 10.1002/adma.202107986.

[8] R. R. Arvizo, S. Bhattacharyya, R. A. Kudgus, K. Giri, R. Bhattacharya, și P. Mukherjee, „Intrinsic therapeutic applications of noble metal nanoparticles: past, present and future”, *Chem. Soc. Rev.*, vol. 41, nr. 7, p. 2943, 2012, doi: 10.1039/c2cs15355f.

[9] A. Sati, T. N. Ranade, S. N. Mali, H. K. Ahmad Yasin, și A. Pratap, „Silver Nanoparticles (AgNPs): Comprehensive Insights into Bio/Synthesis, Key Influencing Factors, Multifaceted Applications, and Toxicity─A 2024 Update”, *ACS Omega*, vol. 10, nr. 8, pp. 7549–7582, mar. 2025, doi: 10.1021/acsomega.4c11045.

[10] D. Cialla-May, M. Schmitt, și J. Popp, „Theoretical principles of Raman spectroscopy”, *Physical Sciences Reviews*, vol. 4, nr. 6, iun. 2019, doi: 10.1515/psr-2017-0040.

[11] B. P. Nanda, P. Rani, P. Paul, Aman, S. S. Ganti, și R. Bhatia, „Recent trends and impact of localized surface plasmon resonance (LSPR) and surface-enhanced Raman spectroscopy (SERS) in modern analysis”, *Journal of Pharmaceutical Analysis*, vol. 14, nr. 11, p. 100959, nov. 2024, doi: 10.1016/j.jpha.2024.02.013.

[12] S.-Y. Ding, E.-M. You, Z.-Q. Tian, și M. Moskovits, „Electromagnetic theories of surface-enhanced Raman spectroscopy”, *Chemical Society Reviews*, vol. 46, nr. 13, pp. 4042–4076, 2017, doi: 10.1039/C7CS00238F.

[13] X. X. Han, R. S. Rodriguez, C. L. Haynes, Y. Ozaki, și B. Zhao, „Surface-enhanced Raman spectroscopy”, *Nat Rev Methods Primers*, vol. 1, nr. 1, pp. 1–17, ian. 2022, doi: 10.1038/s43586-021-00083-6.

[14] I. Chaudhry, G. Hu, H. Ye, și L. Jensen, „Toward Modeling the Complexity of the Chemical Mechanism in SERS”, *ACS Nano*, vol. 18, nr. 32, pp. 20835–20850, aug. 2024, doi: 10.1021/acsnano.4c07198.

[15] P. C. Lee și D. Meisel, „Adsorption and surface-enhanced Raman of dyes on silver and gold sols”, ACS Publications. Data accesării: 16 octombrie 2024. [Online]. Disponibil la: https://pubs.acs.org/doi/pdf/10.1021/j100214a025

[16] D. Semeniak, D. F. Cruz, A. Chilkoti, și M. H. Mikkelsen, „Plasmonic Fluorescence Enhancement in Diagnostics for Clinical Tests at Point-of-Care: A Review of Recent

Technologies", *Advanced Materials*, vol. 35, nr. 34, p. 2107986, 2023, doi: 10.1002/adma.202107986.
[17] Q. Zhang, N. Li, J. Goebl, Z. Lu, și Y. Yin, „A Systematic Study of the Synthesis of Silver Nanoplates: Is Citrate a "Magic" Reagent?", *J. Am. Chem. Soc.*, vol. 133, nr. 46, pp. 18931–18939, nov. 2011, doi: 10.1021/ja2080345.
[18] A. Stefancu *et al.*, „Fermi Level Equilibration at the Metal–Molecule Interface in Plasmonic Systems", *Nano Lett.*, vol. 21, nr. 15, pp. 6592–6599, aug. 2021, doi: 10.1021/acs.nanolett.1c02003.
[19] A. M. Chiriac, R. A. Ciceo-Lucacel, S. D. Iancu, și N. Leopold, „Citrate-reduced silver nanoparticles: Synthesis temperature dependent properties", *Applied Surface Science*, vol. 709, p. 163759, nov. 2025, doi: 10.1016/j.apsusc.2025.163759.
[20] „Research-Grade | Confocal Raman Microscope | Distributor", blue-scientific.com. Data accesării: 13 mai 2025. [Online]. Disponibil la: https://blue-scientific.com/products/renishaw/raman-spectroscopy/invia/

Anexa 2

DECLARAȚIE PE PROPRIE RĂSPUNDERE

Subsemnata, Miruna Alexandra Ibrian, declar că Lucrarea de disertație pe care o voi prezenta în cadrul examenului de finalizare a studiilor la Facultatea de Fizică, din cadrul Universității Babeș-Bolyai, în sesiunea de vară 2025 , sub îndrumarea Prof. dr. Nicolae Leopold, reprezintă o operă personală. Menționez că nu am plagiat o altă lucrare publicată, prezentată public sau un fișier postat pe Internet. Pentru realizarea lucrării am folosit exclusiv bibliografia prezentată și nu am ascuns nici o altă sursă bibliografică sau fișier electronic pe care să le fi folosit la redactarea lucrării.

Prezenta declarație este parte a lucrării și se anexează la aceasta.

Data,

23.06.2025

Nume,

Ibrian Miruna Alexandra

Semnătură